

Supplement of Atmos. Chem. Phys., 20, 9581–9590, 2020
<https://doi.org/10.5194/acp-20-9581-2020-supplement>
© Author(s) 2020. This work is distributed under
the Creative Commons Attribution 4.0 License.



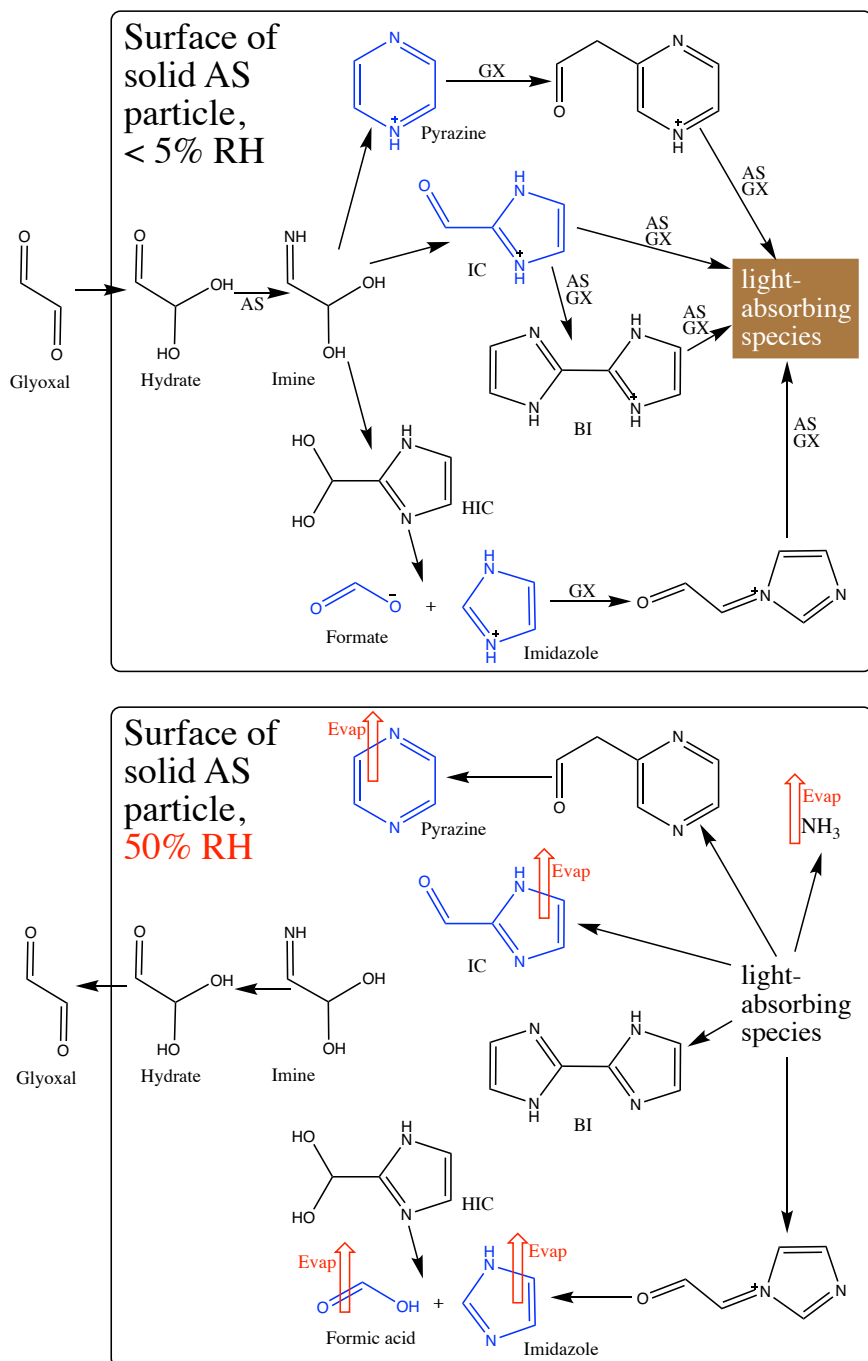
Supplement of

Glyoxal's impact on dry ammonium salts: fast and reversible surface aerosol browning

David O. De Haan et al.

Correspondence to: David O. De Haan (ddehaan@sandiego.edu)

The copyright of individual parts of the supplement might differ from the CC BY 4.0 License.



Scheme S1: Proposed brown carbon formation pathways of glyoxal reacting at solid AS aerosol particle surfaces under dry conditions (top), and response of system to humidification and the associated removal of gas-phase glyoxal (bottom). Aerosol-phase products detected in this study are shown in blue. Formic acid release upon humidification was also detected in the gas phase. IC = 1H-imidazole-2-carboxaldehyde. BI = 2,2'-biimidazole, ref¹. AS = ammonium sulfate. GX = glyoxal.

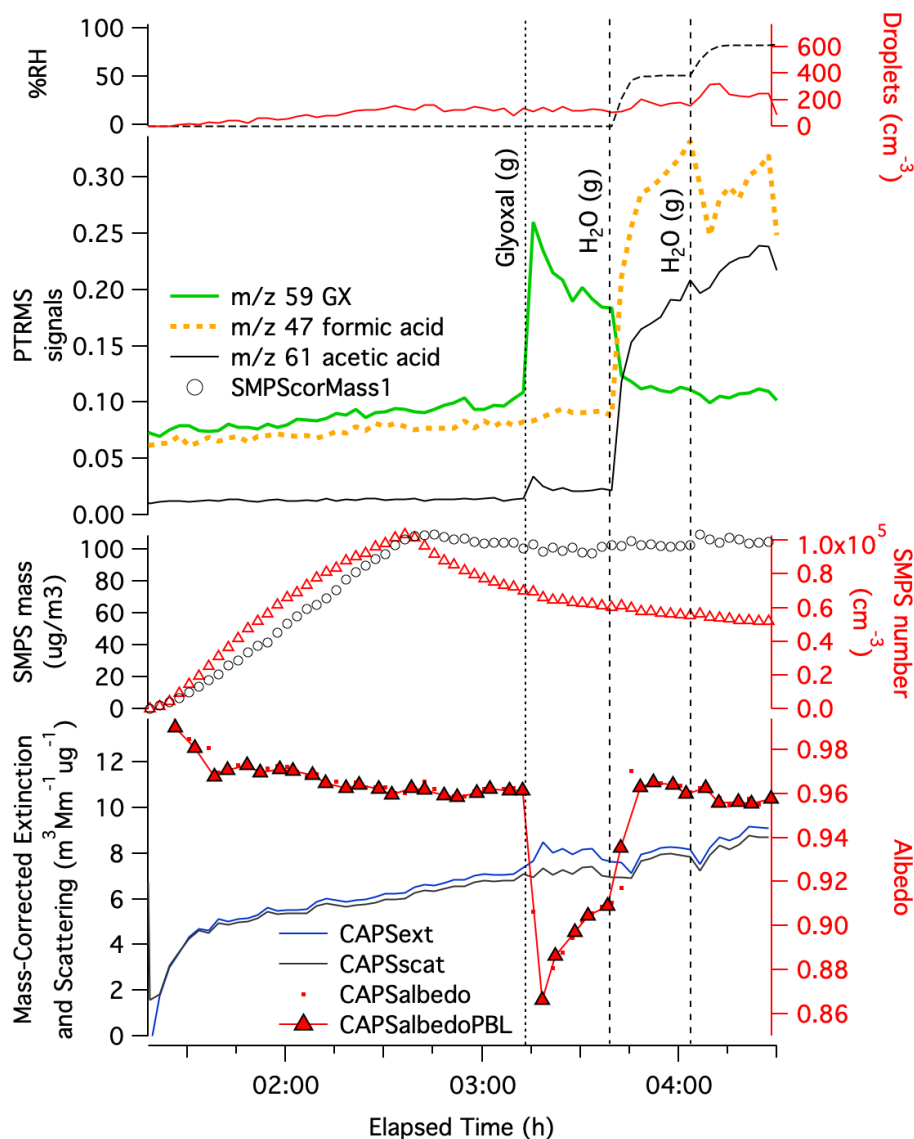


Figure S1: Ammonium sulfate / glycine seed experiment 2. Top: chamber RH and droplet spectrometer counts, traces color-coded to axes. Middle top: dilution- and water-corrected PTR-MS traces are shown for gas-phase glyoxal ($m/z = 59$, green line), formic acid ($m/z = 47$, yellow dotted line), and acetic acid ($m/z = 61$, black line). Middle bottom: dilution-corrected SMPS number density and particulate mass (assuming aerosol density = 1.30) are shown next, with increasing number density indicating internally-mixed AS/glycine aerosol addition at start of experiment. Bottom: mass-normalized 2-min averaged CAPS extinction (blue line), scattering (black line), single-scattering albedo (red dots), and albedo values calculated from data immediately following instrument baseline (red triangles), all measured at 450 nm. Additions of 0.25 ppm glyoxal gas (vertical dotted line), and two water vapor addition (dashed lines) are labeled.

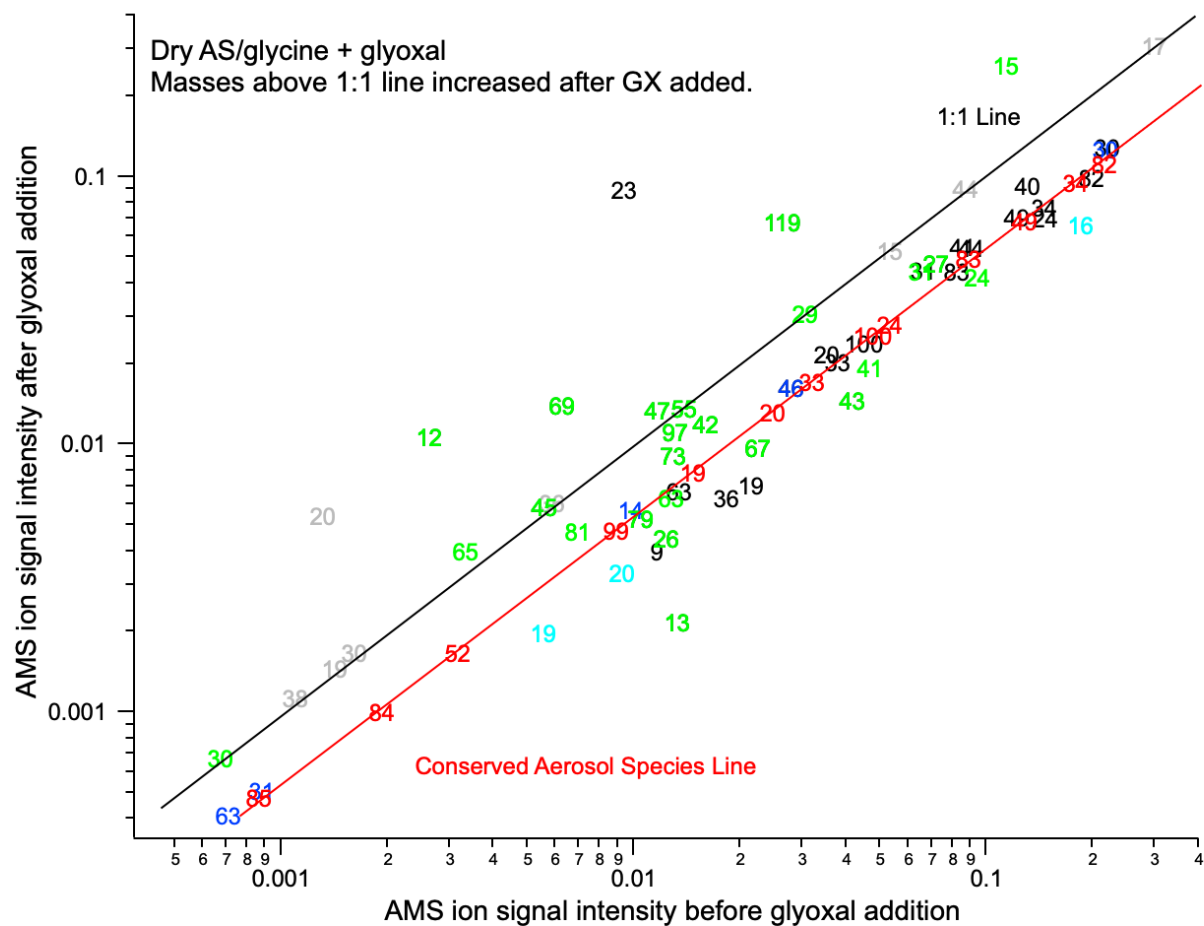


Figure S2: Experiment 3 AMS data summary: dry AS aerosol + 40 ppb glyoxal gas. Overall, aerosol concentrations decreased due to wall losses during the experiment, resulting in ions corresponding to conserved aerosol species falling on the red line with a slope of 1, slightly below the 1:1 line. However, certain ions increased upon GX addition relative to these others and appear above the red line: m/z 15 (CH_3 or NH fragment), 23 (Na), 29 (CHO fragment), 47 (formic acid+ H^+ or a CH_3O_2^+ fragment), 69 (imidazole), 81 (pyrazine), (97 and 119 (imidazole carboxaldehyde, H^+ adduct and sodium adduct, respectively). Ions associated with water (shown in light blue at m/z 16, 19, and 20) declined slightly upon glyoxal addition, appearing below the red line.

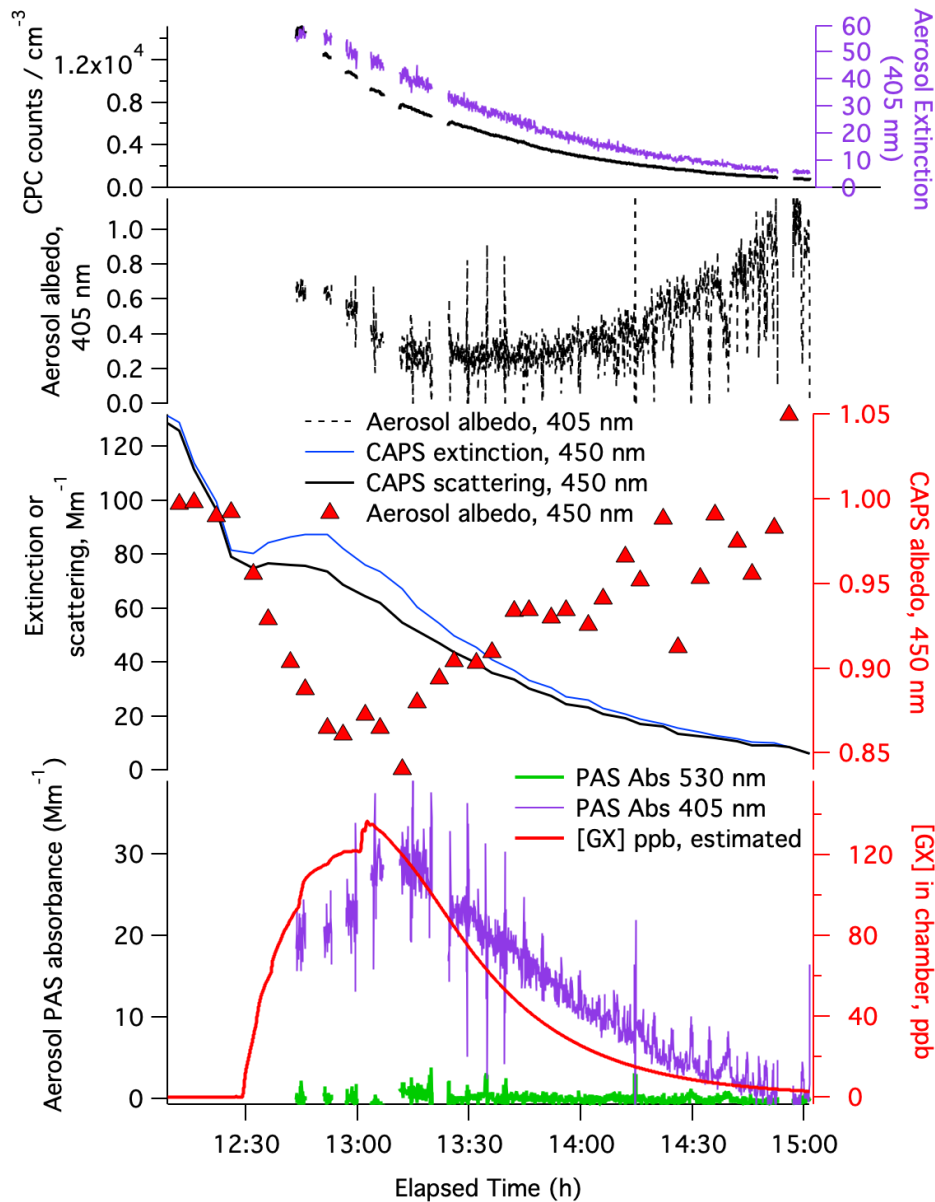


Figure S3: Gradual glyoxal addition experiment 5 on dry MeAS aerosol in small Tedlar chamber. Top: Aerosol CPC counts (black) and CRD extinction at 405 nm (purple). 2nd panel: Aerosol albedo at 405 nm (black dashed line), calculated from PAS and CRD data. 3rd panel: aerosol extinction (blue), scattering (black), and albedo (red triangles), all measured at 450 nm by CAPS-ssa. Bottom: Aerosol absorbance measured by PAS at 405 nm (purple) and 530 nm (green), and estimated glyoxal concentrations in the chamber (red, calculated using wall loss rate = $6.7 \times 10^{-4} \text{ s}^{-1}$). Right axes are color-coded.

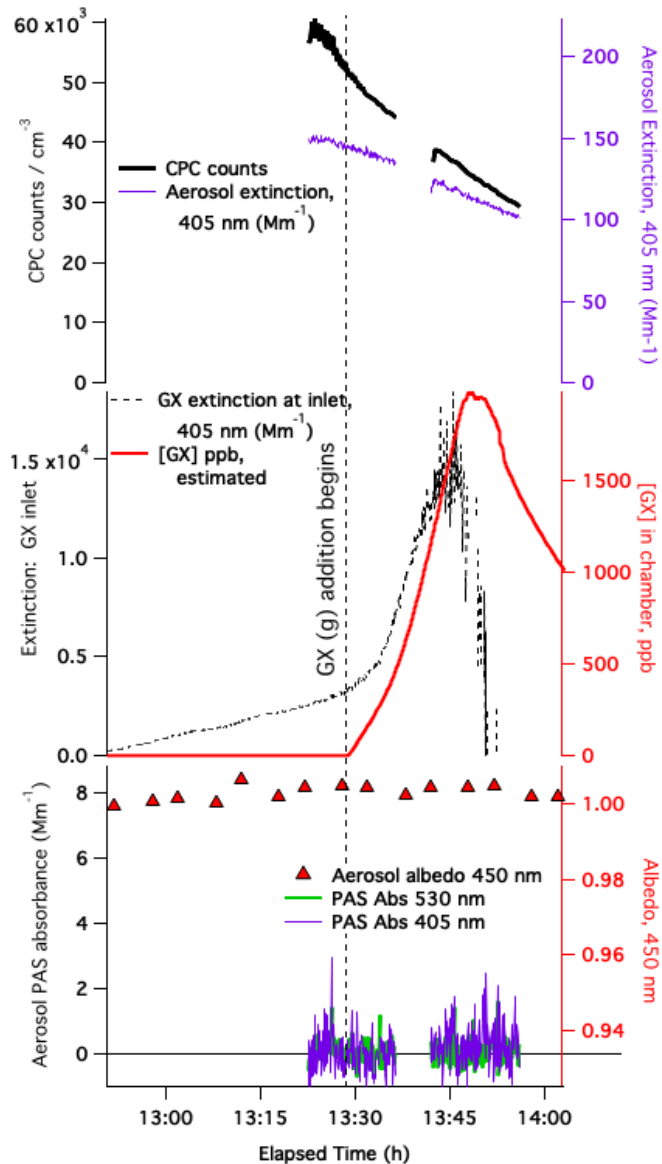


Figure S4: Gradual glyoxal addition experiment 6 on dry sodium sulfate (Na_2SO_4) aerosol in small Tedlar chamber. Top: Aerosol CPC counts (thick black line) and CRD extinction at 405 nm (purple). Middle: CRD extinction at 405 nm due to glyoxal, measured at glyoxal inlet (black dashed line), and estimated glyoxal concentrations in the chamber (red, calculated using wall loss rate = $6.7 \times 10^{-4} \text{ s}^{-1}$). These chamber concentrations (and the glyoxal wall loss rate) were confirmed by measuring glyoxal concentrations by CRD extinction at 405 nm at the chamber outlet at 3 pm. Bottom: CAPS-ssa albedo at 450 nm (red triangles), and aerosol absorbance measured by PAS at 405 nm (purple) and 530 nm (green).

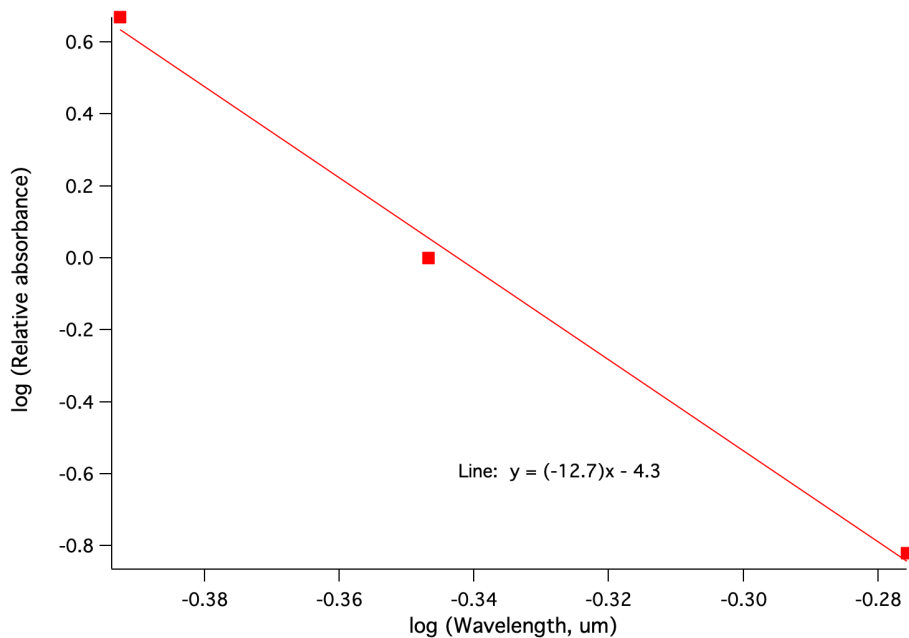


Figure S5: Calculation of angstrom absorption coefficient from normalized aerosol optical data recorded at 405, 450, and 530 nm at 1:11 pm in experiment 5 (140 ppb glyoxal + dry methylammonium sulfate aerosol). Slope of line is Ångstrom absorption coefficient.

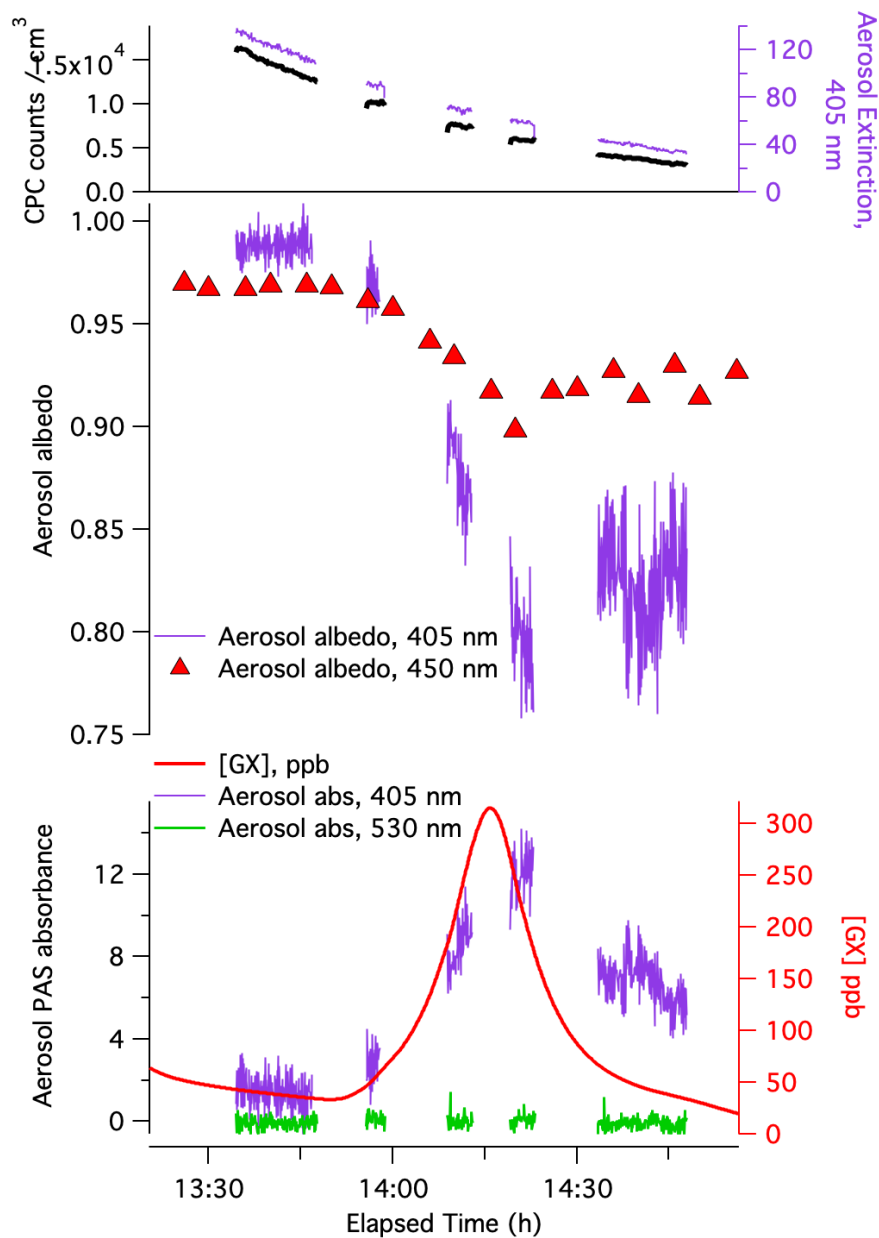


Figure S6: Gradual glyoxal addition experiment 4 on dry ammonium sulfate (AS) aerosol in small Tedlar chamber. Top: Aerosol CPC counts (black) and CRD extinction at 405 nm (purple). Middle: Aerosol albedo at 405 nm (purple), calculated from PAS and CRD data, and aerosol albedo at 450 nm (red triangles) measured by CAPS-ssa. Bottom: Aerosol absorbance measured by PAS at 405 nm (purple) and 530 nm (green), and estimated glyoxal concentrations in the chamber (red, calculated using wall loss rate = $2.7 \times 10^{-3} \text{ s}^{-1}$ onto cleaned Tedlar). Right axes are color-coded.

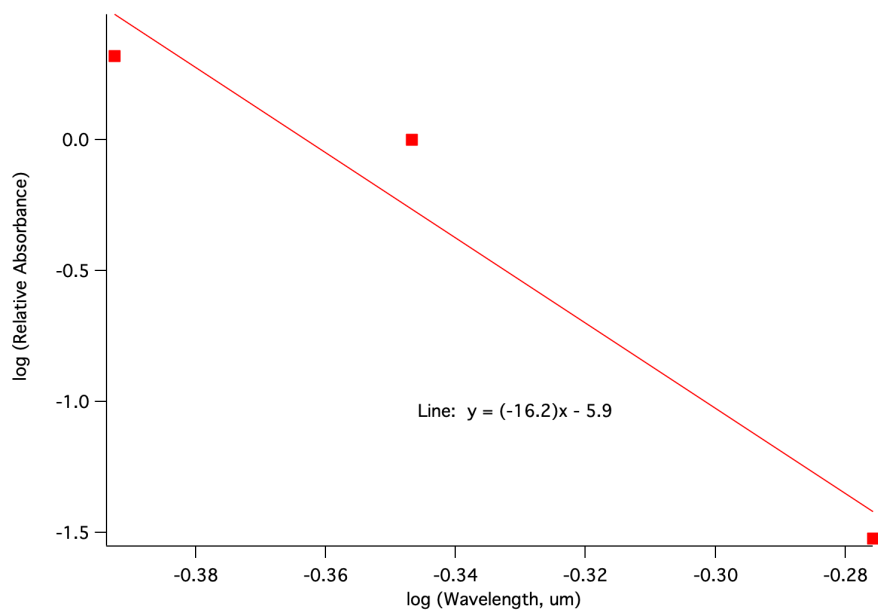


Figure S7: Calculation of angstrom absorption coefficient from normalized aerosol optical data recorded at 405, 450, and 530 nm at 2:20 pm in experiment 4 (300 ppb glyoxal + dry AS aerosol). Slope of line is Ångstrom absorption coefficient.

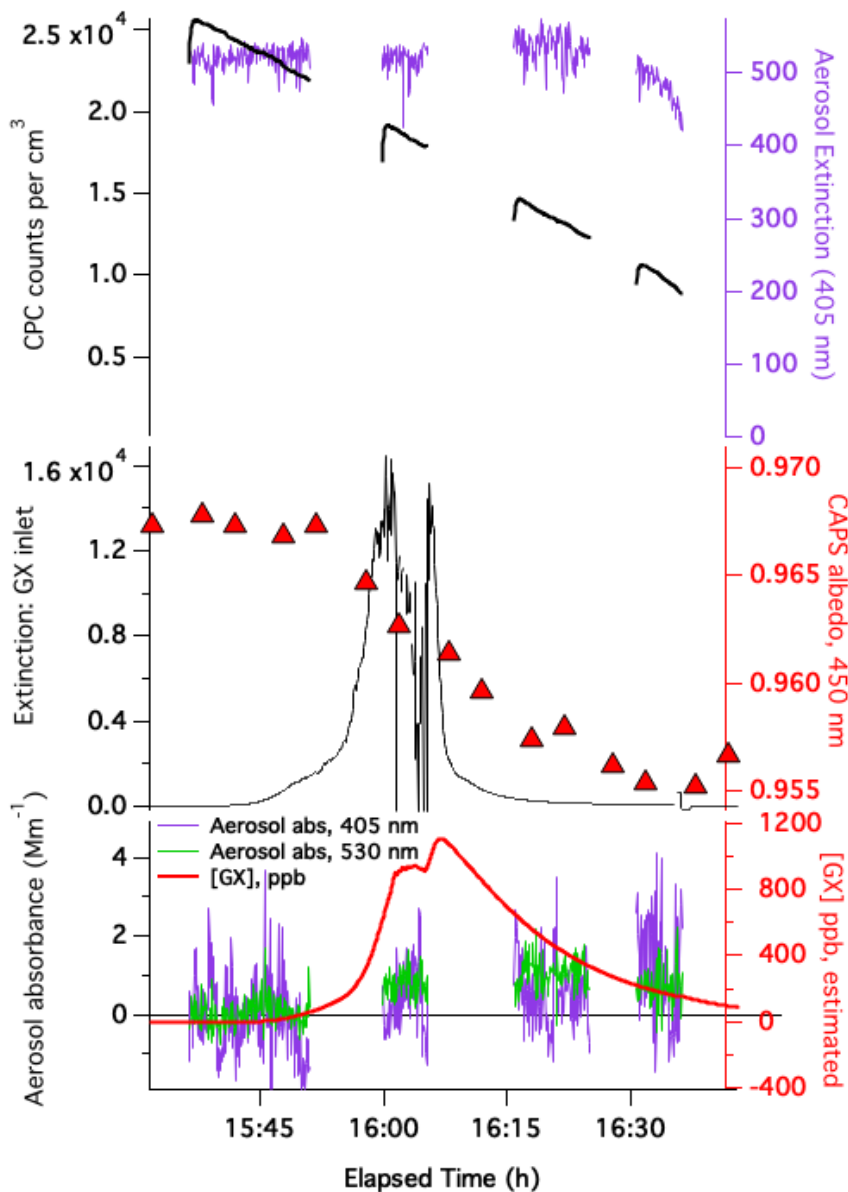


Figure S8: Gradual glyoxal addition experiment 7 on deliquesced ammonium sulfate (AS) aerosol in small Tedlar chamber. Top: Aerosol CPC counts (black) and CRD extinction at 405 nm (purple). Middle: Aerosol albedo at 450 nm (red triangles) measured by CAPS-ssa and glyoxal extinction measured at chamber inlet by CRD at 405 nm (black). Bottom: Aerosol absorbance measured by PAS at 405 nm (purple) and 530 nm (green), and estimated glyoxal concentrations in the chamber (red, calculated using wall loss rate = $1.3 \times 10^{-3} \text{ s}^{-1}$ onto humid Tedlar). Right axes are color-coded.

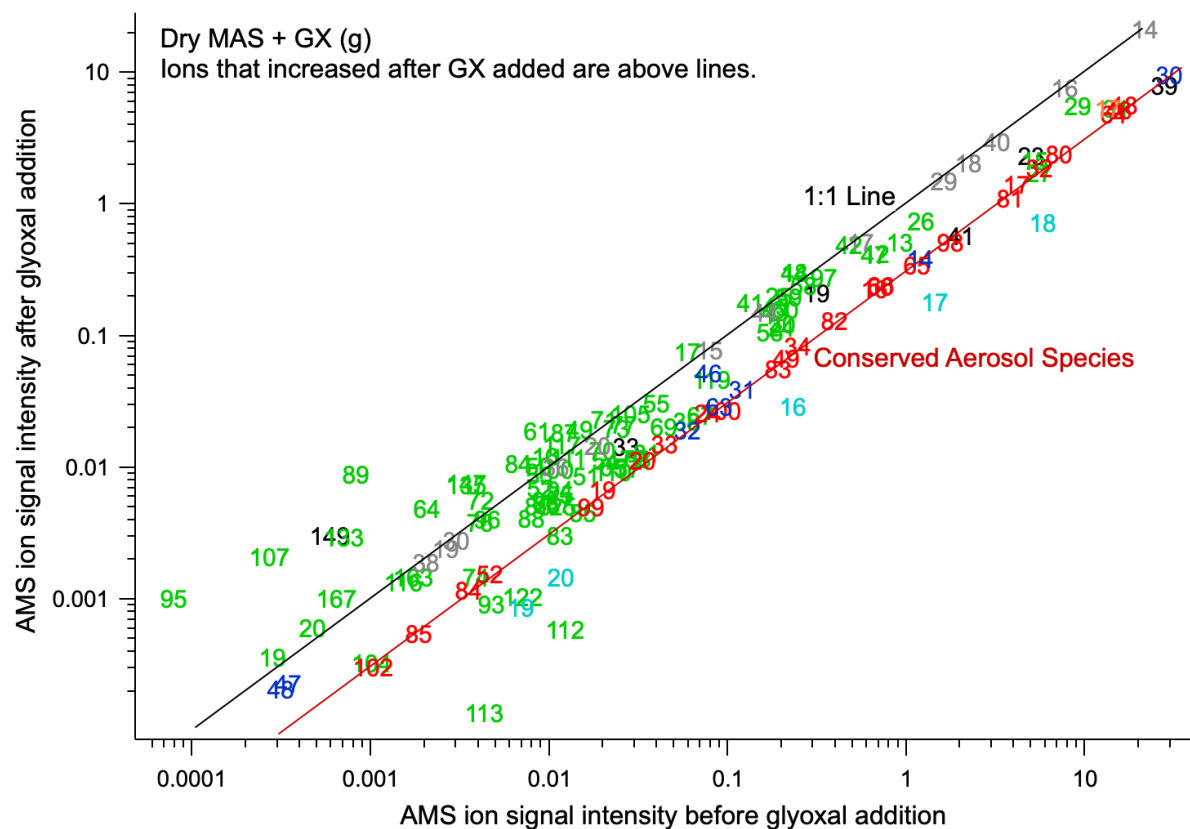


Figure S9: Experiment 5 AMS data summary: dry MeAm₂SO₄ aerosol + 140 ppb glyoxal gas. Overall, aerosol concentrations decreased due to wall losses during the experiment, resulting in ions corresponding to conserved aerosol species falling on the red line with a slope of 1, slightly below the 1:1 line. However, certain ions increased upon GX addition and appear above the red line: *m/z* 29 (GX fragment CHO), 26 (CN), 42 and 97 (dimethylimidazole), among many others, while water peaks decreased at *m/z* 16, 17, and 18.

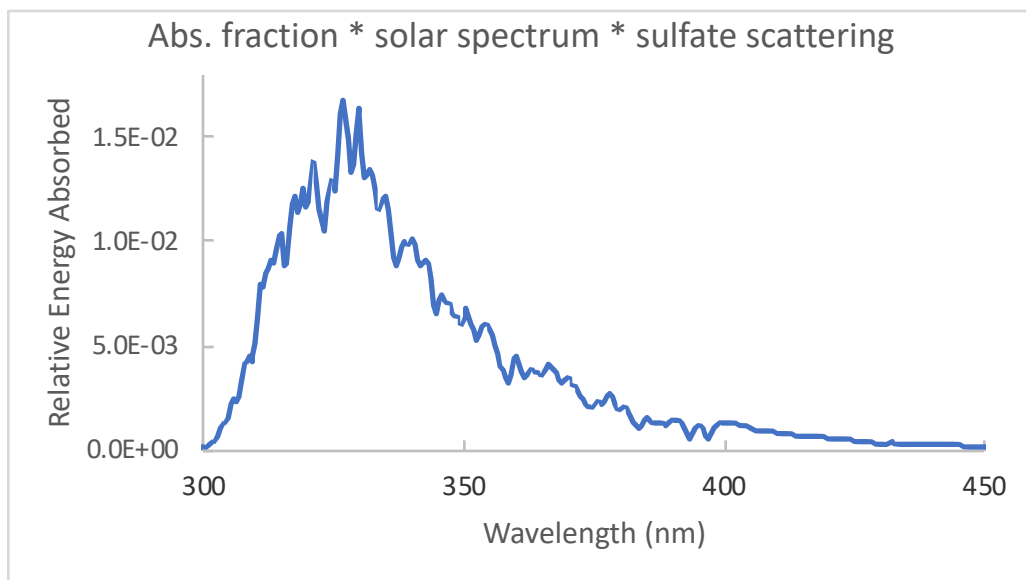


Figure S10: The relative energy absorbed by glyoxal + AS “dry” brown carbon is the calculated product of brown carbon absorbance fraction spectrum (using measured Ångstrom absorbance coefficient = -16), ASTM G173-03 standard solar spectrum, and the AS aerosol scattering function.² Approximately 97% of the energy absorbed by this brown carbon is in the UV range (< 400 nm).

References

1. Kampf, C. J.; Jakob, R.; Hoffmann, T., Identification and characterization of aging products in the glyoxal/ammonium sulfate system -- implications for light-absorbing material in atmospheric aerosols. *Atmos. Chem. Phys.* **2012**, *12*, 6323-6333. doi:10.5194/acp-12-6323-2012
2. Nemesure, S.; Wagener, R.; Schwartz, S. E., Direct shortwave forcing of climate by the anthropogenic sulfate aerosol: Sensitivity to particle size, composition, and relative humidity. *Journal of Geophysical Research: Atmospheres* **1995**, *100*, (D12), 26105-26116. doi:10.1029/95JD02897